Amino Acids (2015) 47:1379–1388
DOI 10.1007/s00726-015-1970-9

ORIGINAL ARTICLE

Chemically functionalized single-walled carbon nanotubes enhance the glutamate uptake characteristics of mouse cortical astrocytes

Manoj K. Gottipati[1] · Elena Bekyarova[2,3] · Robert C. Haddon[4,5] · Vladimir Parpura[1,6]

Received: 18 March 2015 / Accepted: 19 March 2015 / Published online: 3 April 2015

Abstract Using a radioactive glutamate uptake assay and immunolabeling, we report that single-walled carbon nanotubes, chemically functionalized with polyethylene glycol (SWCNT-PEG), delivered as a colloidal solute, cause an increase in the uptake of extracellular glutamate by astrocytes and an increase in the immunoreactivity of the glutamate transporter GLAST on their cell surface, which is likely a consequence of an increase in the immunoreactivity of glial fibrillary acidic protein. Additional corollary is that astrocytes exposed to SWCNT-PEG became larger and stellate, morphological characteristics of maturation and heightened activity of these glial cells. These results imply that SWCNT-PEG could potentially be used as a viable candidate for neural prosthesis applications, perhaps to alleviate the death toll of neurons due to glutamate excitotoxicity, a pathological process observed in brain and spinal cord injuries.

Keywords Carbon nanotubes · Astrocytes · Glial fibrillary acidic protein · Glutamate excitotoxicity

Abbreviations

CNT	Carbon nanotube
EAAT	Excitatory amino acid transporter
GFAP	Glial fibrillary acidic protein
GLAST	L-Glutamate/L-aspartate transporter
GLT-1	Glial L-glutamate transporter
ICC	Indirect immunocytochemistry
ir	Immunoreactivity
PEG	Polyethylene glycol
ROCK	Rho-associated protein kinase
SWCNT	Single-walled carbon nanotube
TBOA	DL-Threo-β-benzyloxyaspartic acid

Introduction

Carbon nanotubes (CNTs) with their unique physical and chemical properties hold much promise in biomedical applications, especially in the field of neuroprosthetics (Bekyarova et al. 2005; Malarkey and Parpura 2007).

Handling Editor: G. Lubec.

Electronic supplementary material The online version of this article (doi:10.1007/s00726-015-1970-9) contains supplementary material, which is available to authorized users.

✉ Vladimir Parpura
vlad@uab.edu

Robert C. Haddon
robert.haddon@ucr.edu

[1] Department of Neurobiology and Department of Biomedical Engineering, University of Alabama at Birmingham, 1719 6th Ave S, CIRC 429, Birmingham, AL 35294, USA

[2] Department of Chemistry and Department of Chemical Engineering, Center for Nanoscale Science and Engineering, University of California, 104 Pierce Hall Annex, Riverside, CA 92521, USA

[3] Carbon Solutions, Inc., Riverside, CA 92507, USA

[4] Department of Chemistry and Department of Chemical Engineering, Center for Nanoscale Science and Engineering, University of California, 203 Pierce Hall Annex, Riverside, CA 92521, USA

[5] Department of Physics, King Abdulaziz University, Jeddah 21589, Saudi Arabia

[6] Department of Biotechnology, University of Rijeka, 51000 Rijeka, Croatia

Single-walled carbon nanotubes, chemically functionalized with polyethylene glycol (SWCNT-PEG) to render their water solubility, have been used in cell culture to modulate the morpho-functional properties of neurons and astrocytes. This nanomaterial promoted the outgrowth of selected neurites (Ni et al. 2005), due to the exocytotic incorporation of vesicles into the plasma membrane which was unbalanced by their endocytotic retrieval (Malarkey et al. 2008). It also made astrocytes larger and stellate along with an increase in the immunoreactivity of glial fibrillary acidic protein (GFAP) (Gottipati et al. 2012), an astrocyte-specific intermediate filament; the resulting cellular characteristics render a mature astrocyte phenotype. An application of SWCNT-PEG in vivo at the site of an acute spinal cord injury also showed an alteration in neuronal morphology and an improvement in the locomotor recovery in a rat model (Roman et al. 2011). While these findings implicate the potential beneficial effects of CNTs at the injury site, the possible effects on astrocytes and the contribution of these glial cells is this process were not detailed. Namely, an additional concern with an injury to the spinal cord is the 'secondary injury' which leads to progressive degenerative events at the site of the injury (Park et al. 2004). One of the prominent mechanisms that lead to secondary injury is excitotoxicity, a pathological process that results in the death of neurons due to excessive stimulation by glutamate. Astrocytes are the main brain element responsible for the uptake of excess glutamate from the extracellular space through their Na^+-dependent excitatory amino acid transporters (EAATs), assuring the fidelity of synaptic transmission and protecting the neighboring neurons. Since the loss of GFAP has been implicated in the trafficking of glutamate transporters to the plasma membrane (Hughes et al. 2004), the question arose whether an increase in GFAP caused by the CNTs could be associated with an increase in the trafficking of the glutamate transporters to the cell surface, resulting in an increased glutamate uptake; this is the very subject of the present study.

CNTs found use in brain machine interface applications as a coating material for implantable electrodes. CNT surface coating has shown to outperform the traditional tungsten and stainless steel wire electrodes by improving the electrical stimulation of neurons and recordings from these cells (Keefer et al. 2008). However, whether CNTs, by acting on astrocytic uptake mechanism, could help in reducing the transient increase in glutamate levels that otherwise occurs following a microelectrode implantation (Chang et al. 2009) is untested.

We performed a radioactive glutamate uptake study and immunolabeling to show that the CNT-treated astrocytes have an enhanced capacity to uptake glutamate from the extracellular space, a functional output of an increased presence of the glutamate transporters on their surface; this CNT-mediated modulation of glutamate uptake was associated with astrocytes assuming a more mature morphological (larger and stellate shape) and functional (increased expression of GFAP) phenotype. Taken together, these findings further emphasize the potential of CNTs as a viable candidate for neuroprosthesis applications.

Materials and methods

Ethical approval

All procedures were in strict accordance with the National Institutes of Health Guide for Care and Use of Laboratory Animals and were approved by the University of Alabama at Birmingham Institutional Animal Care and Use Committee. The procedures also conform to the principles of UK regulations (Drummond 2009).

Purified astrocytic cell culture

Purified astrocytic cultures were made using a modification (Gottipati et al. 2012; Reyes et al. 2011) of the originally described shaking procedure (McCarthy and de Vellis 1980). Briefly, visual cortices were dissected from 0- to 2-day-old C57BL/6 mice pups and treated with papain in the presence of L-cysteine, neutralized with trypsin inhibitor and triturated in cell culture medium containing α-minimum essential medium (without phenol red; Invitrogen) supplemented with fetal bovine serum (10 %, Hyclone), sodium bicarbonate (14 mM), sodium pyruvate (1 mM), D-glucose (20 mM), L-glutamine (2 mM), penicillin (100 IU/ml) and streptomycin (100 μg/ml) (pH 7.35). The resulting cell suspension was applied into 25 cm^2 tissue culture flasks and maintained at 37 °C in a 5 % CO_2/95 % air incubator. The cells were allowed to grow and proliferate for 7–14 days, until they reached ~60 % confluency, after which the cell cultures were purified for astrocytes using a shaking procedure described elsewhere (Gottipati et al. 2012). The cells attached to the bottom of the flask were detached by adding trypsin and pelleted by centrifugation at 100 g for 10 min. The cells were resuspended in cell culture medium and plated onto polyethyleneimine (PEI; 1 mg/ml)-coated glass coverslips (12 mm in diameter) inlayed in tissue culture dishes, except for the glutamate uptake assay where the cells were plated into 24-well tissue culture plates. Cells were returned to the incubator for 1 h to allow for the attachment of astrocytes to the strata. At this juncture, dishes/plates were rinsed, and PEG (1 μg/ml), SWCNT-PEG (5 μg/ml) or Y-27632 (30 μM), diluted in the cell culture medium, was applied to the astrocytes, which were then returned to the incubator until used in the experiments.

Modification of carbon nanotubes

SWCNT-PEG solute was synthesized and characterized as we previously reported in detail elsewhere (Gottipati et al. 2012). The batch of SWCNT-PEG solute used in this study contained 72.3 weight percent (wt%) of the SWCNT backbone, 22.6 wt% of the functional group PEG and 5.1 wt% of metal impurities (nickel and yttrium in ~4:1 weight ratio; Online Resource 1, Fig. S1). In the experiments using the functional group PEG alone, as a control for 5 μg/ml of SWCNT-PEG solute-treated group, PEG was added to the cells at 1 μg/ml, i.e., at the concentration corresponding to 20 wt% of the SWCNT-PEG solute.

[^{3}H]-L-glutamate uptake assay

Glutamate uptake assay was done using a procedure described elsewhere (Aprico et al. 2004). Briefly, astrocytes plated in the 24-well plates were washed twice with Na^+-dependent uptake buffer composed of (in mM): NaCl (135), KCl (5), $CaCl_2$ (1), $MgSO_4$ (0.6), D-glucose (6) and HEPES (10) (pH 7.4). After two washes, the uptake buffer was supplemented with 100 μM of L-glutamate, a mixture of [^{3}H]-L-glutamate (American Radiolabeled Chemicals, Saint Louis, MO) and nascent L-glutamate in a ratio of 1:1500. After 5 min, the solution (containing glutamate) in the wells was replaced with ice-cold phosphate-buffered saline (PBS) to stop the uptake of glutamate; PBS solution was composed of (in mM): NaCl (137), KCl (2.7), Na_2HPO_4 (10) and KH_2PO_4 (1.8) (pH 7.2). Cells were then lysed with NaOH (0.3 M) for 30 min at 37 °C, which was neutralized with HCl (0.3 M). The lysate was analyzed for both [^{3}H]-L-glutamate and protein contents. The radioactivity of [^{3}H]-L-glutamate in an aliquot of each of the samples was measured using a Beckman LS 6500 scintillation counter; these measurements were taken upon dilution of the sample in the ScintiVerse BD Cocktail (Fisher Scientific, Pittsburgh, PA). The remaining lysate was used to measure the total protein concentration of cells in each of the wells using a spectrophotometer. Proteins were quantified using the Bradford reagent (Pierce Biotechnology, Rockford, IL, USA) and bovine serum albumin as a standard. The radioactivity and the total protein concentration were used to calculate the amount of glutamate (in nmol) taken up by the astrocytes per mg of protein per minute. All the measurements are normalized to the average glutamate uptake obtained from the control/untreated astrocytes and reported.

Live cell imaging

The morphology of live astrocytes was examined as previously described (Gottipati et al. 2012; Hua et al. 2004). Coverslips with astrocytes were incubated with the non-fluorescent calcein acetoxymethyl ester (AM) (1 μg/ml; Invitrogen) at room temperature (RT; 22–25 °C) for 15 min; 0.025 % (w/v) pluronic acid (Invitrogen) was added to aid in the solubilization of calcein AM in external solution containing (in mM) NaCl (140), KCl (5), $CaCl_2$ (2), $MgCl_2$ (2), D-glucose (5) and HEPES (10) (pH 7.4). After rinsing, cells were kept for another 15 min in external solution to allow for the de-esterification of calcein AM, resulting in the intracellular accumulation of calcein, a vital fluorescent dye. These coverslips were rinsed in external solution and mounted onto an imaging chamber filled with external solution. We examined cells using an inverted microscope (Nikon TE300) equipped with differential interference contrast (DIC; 100-W halogen lamp) and wide-field epifluorescence illumination (100-W xenon arc lamp). Visualization was accomplished using a standard fluorescein isothiocyanate (FITC; Chroma Technology Corp.) filter set and a 60X Plan Apo objective and imaged using a CoolSNAP®-HQ^2 cooled charge-coupled device (CCD) camera (Roper Scientific Inc.) driven by V++ imaging software (Digital Optics, Auckland, New Zealand). Neutral density filters and an electronic shutter (Vincent Associates, Rochester, NY), controlled by the software, were inserted in the excitation pathway to reduce photo-bleaching.

Morphometric analysis

Acquired calcein images were analyzed to get the morphometric parameters of the cells as described in detail elsewhere (Gottipati et al. 2012). Briefly, two or more images were processed by image stitching and auto-leveling, when the cell size exceeded an individual image frame. Images were processed using a 3 × 3 kernel, which is a low-pass filter, to reduce the effect of noise along the perimeter. A Laplacian of Gaussian (LoG) 3D filter (Sage et al. 2005) was then applied to images to facilitate edge detection. A circle containing octants was centered over the astrocyte in the LoG3D image, and regions of interest (10 × 10 pixels) were created at the intersections of the octant radii and the cell edge/perimeter. These regions were transposed onto the kernel-filtered image, the average intensities of the regions were calculated, which were further averaged, and the resulting overall mean intensity was used as the intensity threshold value applied to the very image. Based on the intensity threshold, the outline of the cell was obtained and used to calculate the area and perimeter values, which were further used to calculate the form factor (FF) for each of the cells using equation 1 (Wilms et al. 1997):

$$\mathrm{FF} = 4\pi \left[\mathrm{area}\left(\mu\mathrm{m}^2\right)\right] \Big/ \left[\mathrm{perimeter}\ (\mu\mathrm{m})\right]^2 \quad (1)$$

Indirect immunocytochemistry (ICC) and analysis

Immunolabeling of astrocytes was done using previously described procedures (Gottipati et al. 2012; Hua et al. 2004; Montana et al. 2004). Coverslips with astrocytes were fixed at RT for 30 min with freshly prepared Dent's fixative (80 % methanol, 20 % dimethyl sulfoxide) for GFAP or with 4 % paraformaldehyde for L-glutamate/L-aspartate transporter (GLAST/EAAT1; SLC1A3) and glial L-glutamate transporter (GLT-1/EAAT2; SLC1A2); this was followed by permeabilization of the cells using 0.25 % Triton X-100 for 10 min. To prevent non-specific binding of antibodies, the cells were then incubated with 10 % (v/v) goat serum in PBS for 30 min followed by 16- to 20-h incubation of the cells at 4 °C with primary antibodies against GFAP (1:500; MP Biomedicals), GLAST (1:250; Alomone Labs) or GLT-1 (1:250; Millipore). Cells were then washed thrice with PBS and incubated for 1 h with tetramethylrhodamine isothiocyanate (TRITC)-conjugated secondary (goat anti-mouse for GFAP and GLT-1, or goat anti-rabbit for GLAST) antibody (1:200; Millipore) at RT. To test for the non-specific binding of the secondary antibody, parallel controls were run in which the primary antibodies were omitted. After multiple washings with PBS and Milli-Q® water, the coverslips were mounted onto glass microscopic slides in ProLong® Gold antifade reagent (Invitrogen) to prevent photo-bleaching. For experiments assessing the surface expression of GLAST and a lack of thereof for GFAP, a non-permeabilization procedure was used where the above-described ICC procedure was performed, but with the omission of the detergent, Triton X-100 (Malarkey et al. 2008). Of note, anti-GLAST antibody recognizes the extracellular epitope of this transporter when incorporated into the plasma membrane. Correspondingly, this epitope is located in the lumina of the endoplasmic reticulum and of the GLAST-laden trafficking vesicles; these intracellular locations can be labeled upon the permeabilization of the cell.

Immunoreactivity (ir) was visualized and imaged using a standard TRITC (Chroma Technology Corp.) filter set and the above-mentioned microscope and associated equipment; matching DIC images were also obtained. Analysis was done using Metamorph 7.8 (Molecular Devices, Chicago, IL) to get the total area of the cell, area of the cell occupied by protein-ir and the average intensity or density of protein-ir, which is the intensity of protein-ir per pixel. The DIC images were manually traced along their edge/perimeter to get the total area of the cells. No primary antibody controls were used to calculate the threshold value for the immunolabeled astrocytes, where the background-subtracted mean intensity of the control cells (autofluorescence) + 3 standard deviations (for GLAST and GLT-1) or 6 standard deviations (for GFAP) was used as the threshold value; the background fluorescence was obtained from regions of coverslips containing no cells. The pixels exceeding these threshold values were used to obtain the positive signal and calculate the protein-ir occupancy, which is the ratio of the area of the cell occupied by protein-ir (fluorescence) to the total area (DIC) of the cell, as well as the protein-ir content, which is the product of the average intensity of protein-ir and the total area of the cell. Furthermore, based on the number of the pixels above these threshold values, we classified cells as positive for the specific antigen, i.e., the cells were considered to express a given protein if the number of positive pixels in a cell was at least 1 standard deviation greater than the average number of noise/false-positive pixels observed in the cells that were processed for ICC without the primary antibody. All raw fluorescence images had pixel intensities without saturation and within the camera's dynamic range (0–16383).

Statistical analysis

All the statistical analysis was done using the GB-Stat v6.5 software (Dynamic Microsystems Inc., Silver Spring, MD) and SAS Software, version 9.4, of the SAS software for Windows (SAS Institute Inc., Cary, NC). All the data are reported as means ± standard errors of means (Fig. 1) or medians with their interquartile range (Figs. 2, 3, 4 and Online Resource 1, Fig. S2). The number of subjects required for individual set of experiments was estimated using power analysis and set at 80 % and an $\alpha = 0.05$. Nonparametric statistics were used for the subgroups that deviated from normality based on the Shapiro–Wilk test for normality. For the glutamate uptake assay (Fig. 1), the independent groups were first analyzed using one-way ANOVA followed by the Fisher's least significant difference (LSD) test for multiple comparisons. For the assay estimating the surface GLAST-ir (Fig. 2), as well as for the validation of the (non-)permeabilization procedure using GFAP-ir (Online Resource 1, Fig. S2), the two independent groups were compared using the Mann–Whitney *U* test. For the other experiments assessing the effects of the various treatments on the morphology and GFAP-ir (Figs. 3, 4), the independent groups were first analyzed using the Kruskal–Wallis one-way ANOVA (KWA) followed by the Dunn's test for multiple comparisons.

Results

Mouse neonatal astrocytes express GLAST but not GLT-1: confirmation in the culture system

Astrocytes uptake extracellular glutamate primarily through the excitatory amino acid transporters, GLAST/EAAT1 and GLT-1/EAAT2, present on their surface. The transporter type is developmentally regulated so that early neonatal

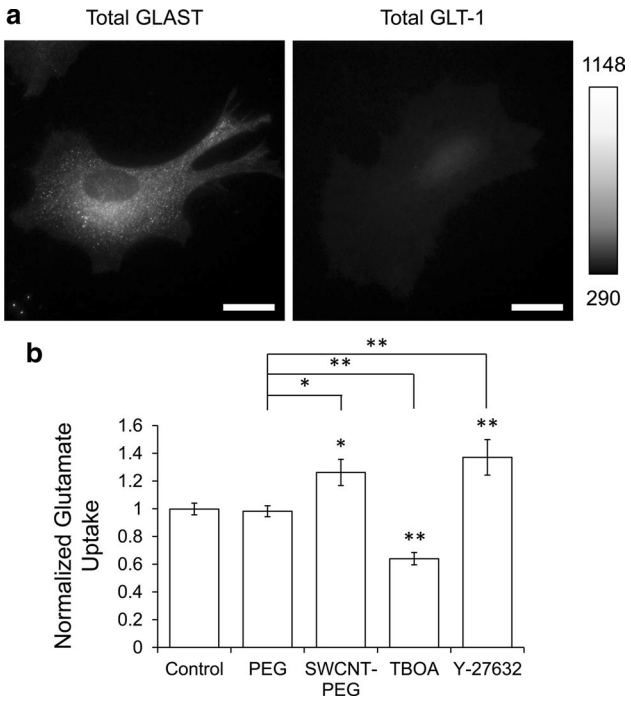

Fig. 1 SWCNT-PEG solute enhances the uptake of [^{3}H]-L-glutamate by mouse cortical astrocytes in culture. **a** Images of astrocytes in culture, labeled for the glutamate transporters GLAST (*left*) and GLT-1 (*right*), using indirect immunocytochemistry. *Scale bar*, 20 µm. *Gray scale* is a linear representation of the fluorescence intensities, expressed in fluorescence intensity units, of the pixels in the images. **b** Summary graph showing the normalized average effect of 1 µg/ml PEG, 5 µg/ml SWCNT-PEG, 100 µM TBOA and 30 µM Y-27632 on the uptake of [^{3}H]-L-glutamate by cultured astrocytes. *Bars* represent means with standard error of means. 18 wells containing astrocytes were analyzed per condition. *Asterisks* indicate a statistical difference compared to the control. Other differences are marked by the *brackets*. One-way ANOVA followed by Fisher's LSD test; *$p < 0.05$, **$p < 0.01$

(1-day-old) rat astrocytes show very low levels of expression of GLT-1 compared to GLAST (Furuta et al. 1997). We confirmed this expression pattern/level in our culture system by labeling mouse astrocytes, plated onto PEI-coated coverslips, for GLAST and GLT-1 using ICC and the permeabilization procedure to allow for the detection of total protein levels. We visualized the transporters-ir and found a significant expression of GLAST ($n = 20$; Fig. 1a, left), while only a faint stain of GLT-1 ($n = 20$; Fig. 1a, right). While all astrocytes were positive for GLAST, only 10 % of the cells analyzed were positive for GLT-1.

SWCNT-PEG upregulates the uptake of [^{3}H]-L-glutamate by astrocytes

To assess whether the treatment of astrocytes with SWCNT-PEG induces a change in the uptake of glutamate from the extracellular space, we treated astrocytes plated into 24-well tissue culture plates with 5 µg/ml of SWCNT-PEG for 4 days; a part of the wells were treated with 1 µg/ml of PEG alone to determine whether the functional group by itself has any effect on the uptake of glutamate. To show that the uptake of glutamate can indeed be upregulated in culture, a part of the wells were treated for 2 days with 30 µM of Y-27632, a Rho-associated protein kinase (ROCK) blocker known to cause rapid and reversible stellation of astrocytes and an increase in the uptake of glutamate (Abe and Misawa 2003; Lau et al. 2011). On the day of the experiment, all the wells were incubated in a Na^+-dependent uptake buffer containing a 100 µM glutamate mixture ([^{3}H]-L-glutamate and nascent glutamate in a ratio of 1:1500) for 5 min. A part of the untreated wells incubated with the glutamate mixture were additionally exposed to 100 µM of DL-threo-β-benzyloxyaspartic acid (TBOA), which is a competitive, non-transportable EAAT blocker (Shimamoto et al. 1998). The amount of radioactive glutamate taken up by the astrocytes was estimated using a scintillation counter. Expectedly, we found that TBOA significantly blocked the uptake of glutamate (~40 % reduction in the uptake), while the positive control, Y-27632, caused a significant increase compared to the control (Fig. 1b; one-way ANOVA followed by Fisher's LSD test). The cells treated with SWCNT-PEG, but not PEG alone, showed a significant increase in the uptake of radioactive glutamate (Fig. 1b).

SWCNT-PEG causes an increase in the immunoreactivity of GLAST present on the plasma membrane of astrocytes

Since SWCNT-PEG caused an increase in the uptake of glutamate from the extracellular space, and since GLAST is the predominantly expressed glutamate transporter in neonatal astrocytes, we studied whether the CNT effect on glutamate uptake could be due to an altered amount of GLAST protein present on the plasma membrane of the astrocytes using ICC and the non-permeabilization procedure. We first validated our non-permeabilization procedure by using an antibody against GFAP, an intracellular antigen, and comparing the GFAP-ir between the permeabilized and non-permeabilized cells (Online Resource 1, Fig. S2A). We calculated the density of GFAP-ir and found that the cells permeabilized with Triton X-100 showed a strong staining, while the GFAP stain was essentially absent in the non-permeabilized cells (Online Resource 1, Fig. S2B; Mann–Whitney *U* test), indicating that the omission of Triton X-100 from the ICC procedure leaves the plasma membrane intact, i.e., impermeable for antibodies.

Next, astrocytes plated onto PEI-coated coverslips were treated with 5 µg/ml of SWCNT-PEG for 4 days and labeled for GLAST using ICC and the non-permeabilization

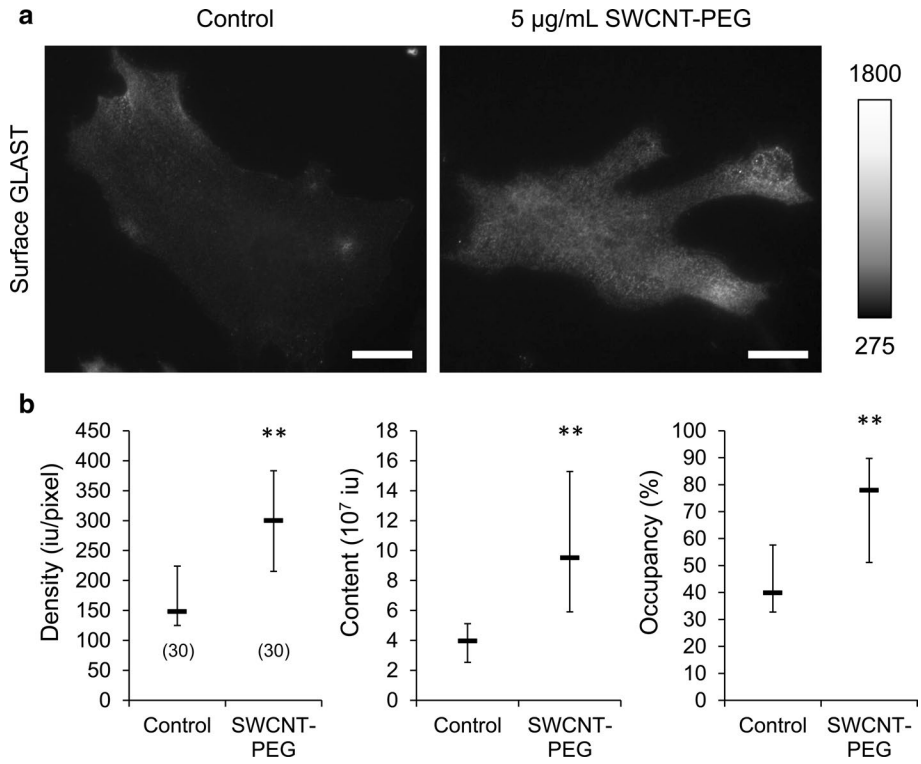

Fig. 2 SWCNT-PEG solute increases the surface appearance of GLAST on mouse cortical astrocytes. **a** Images of astrocytes in culture, a subset of which were treated with 5 µg/ml SWCNT-PEG, labeled for GLAST using indirect immunocytochemistry and the non-permeabilization procedure. *Scale bar*, 20 µm. *Gray scale* is a linear representation of the fluorescence intensities, expressed in fluorescence intensity units (iu), of the pixels in the images. **b** Summary graphs showing the median effect of SWCNT-PEG on the quantitative GLAST immunoreactivity (ir) parameters, i.e., density, content and occupancy. Density is shown in fluorescence iu per area (*pixel*). *Boxes* represent medians with interquartile range. *Number* of astrocytes studied in each condition is given in parentheses in the density graph. *Asterisks* indicate a statistical difference when compared to the untreated/control astrocytes. Mann–Whitney *U* test. $^{**}p < 0.01$

procedure (Fig. 2a). We quantitatively assessed the surface GLAST-ir parameters, that is, density, content and occupancy and found a significant increase in all the parameters in the presence of SWCNT-PEG (Fig. 2b; Mann–Whitney *U* test) implying that the CNTs cause an increase in the amount of GLAST protein present on the surface/plasma membrane of the astrocytes, which likely explains the increase in glutamate uptake caused by SWCNT-PEG.

SWCNT-PEG and Y-27632 increase the immunoreactivity of GFAP in astrocytes

The loss of GFAP has been shown to hamper the trafficking of EAAT2 to the cell surface (Hughes et al. 2004). Consequently, we investigated whether this increase in the surface GLAST presentation by SWCNT-PEG is correlated to an increase in GFAP levels. To assess the effects of the various treatments on GFAP levels, we plated astrocytes onto PEI-coated coverslips in all the conditions used above for the glutamate uptake study and labeled them for GFAP using ICC (Fig. 3a). We quantitatively assessed the GFAP-ir parameters and found that SWCNT-PEG causes a significant increase in all the ir parameters measured, while PEG alone did not cause any significant changes compared to the untreated astrocytes (Fig. 3b; KWA followed by Dunn's test); these findings are consistent with our previous work (Gottipati et al. 2014). Y-27632 also caused a significant increase in all the GFAP-ir parameters assessed compared to the untreated astrocytes. Taken together, these results indicate that the increase in glutamate uptake and surface GLAST induced by SWCNT-PEG is accompanied by an increase in GFAP-ir; the latter can be emulated by a ROCK inhibitor.

SWCNT-PEG and Y-27632 cause morphological alterations in astrocytes

Changes in GFAP levels have been associated with the morphological plasticity of astrocytes (Brenner 2014). So, we assessed the morphology of astrocytes in all the conditions used above for the glutamate uptake study. The astrocytes were loaded with calcein and imaged live. We

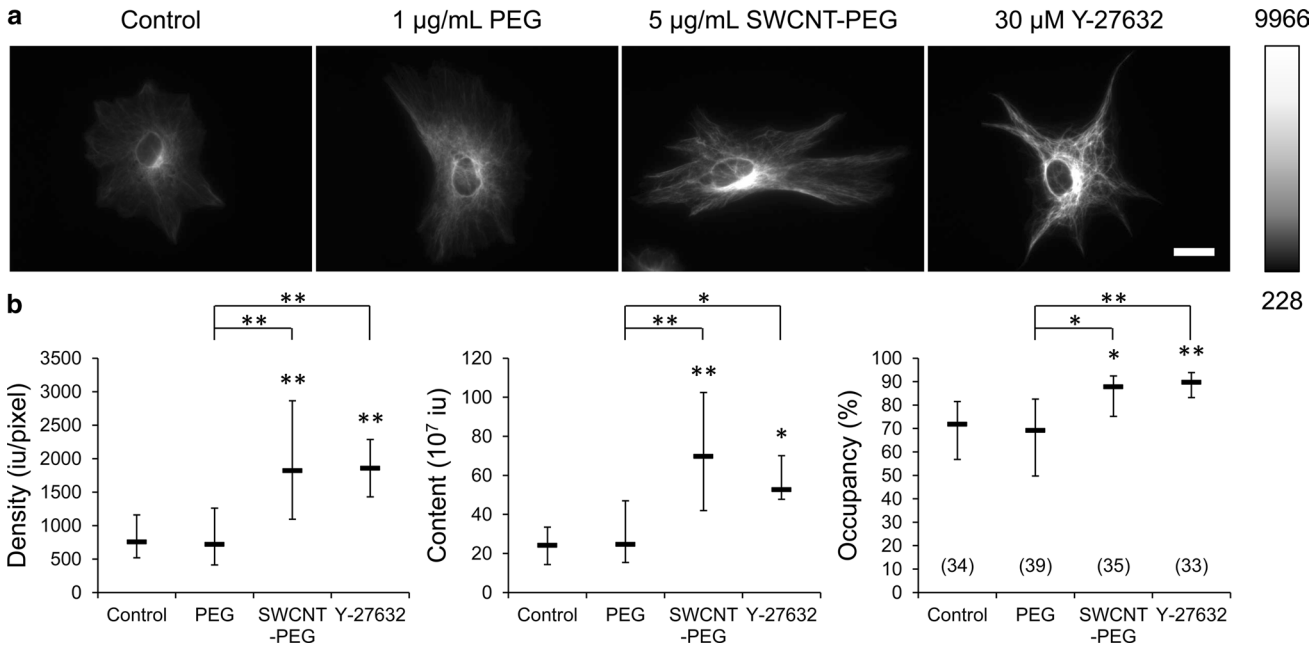

Fig. 3 SWCNT-PEG increases the GFAP-ir parameters in mouse cortical astrocytes. **a** Images of astrocytes in culture, treated with 1 µg/ml PEG, 5 µg/ml SWCNT-PEG or 30 µM Y-27632 and labeled for GFAP using indirect immunocytochemistry. *Scale bar*, 20 µm. **b** Summary graphs showing the median effect of the various treatments on the quantitative GFAP-ir parameters. *Number* of astrocytes studied in each condition is given in parentheses in the occupancy graph. *Asterisks* indicate a statistical difference when compared to the untreated/control astrocytes. Other differences are marked by the *brackets*. Kruskal–Wallis one-way ANOVA (KWA) followed by Dunn's test. *$p < 0.05$, **$p < 0.01$. Other annotations as in Fig. 2

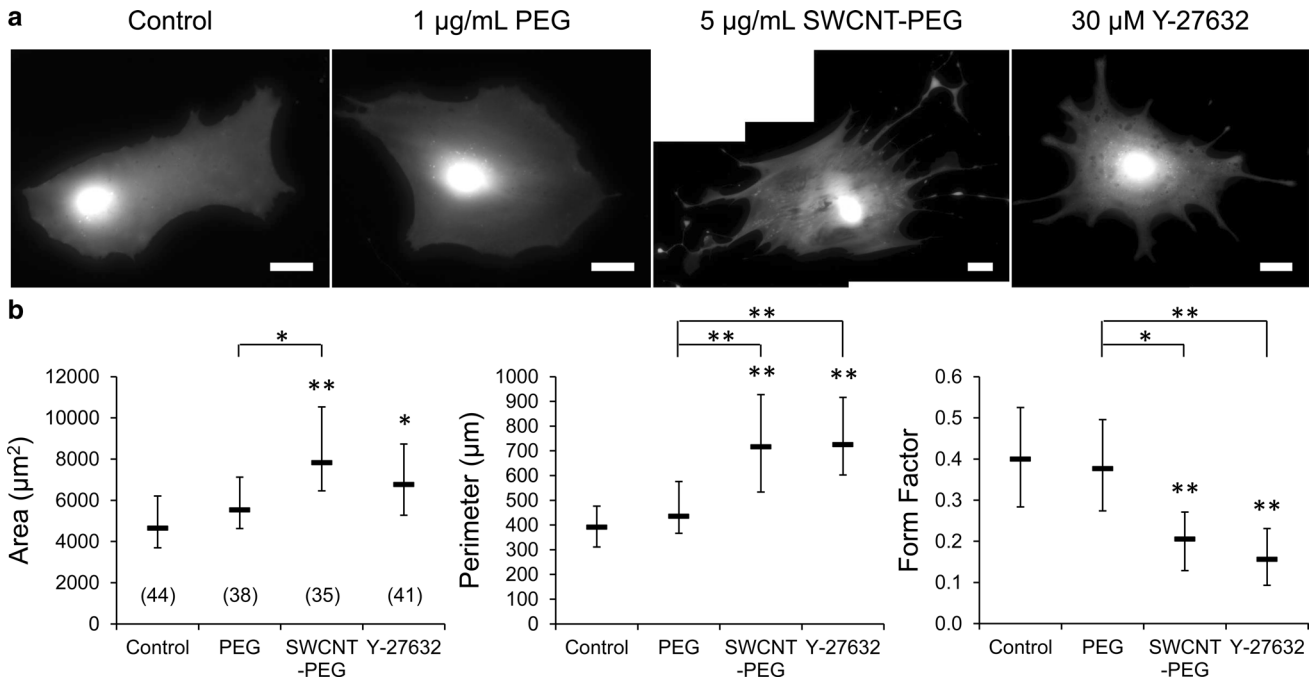

Fig. 4 SWCNT-PEG solute induces morphological changes in mouse cortical astrocytes. **a** Images of astrocytes in culture, treated with 1 µg/ml PEG, 5 µg/ml SWCNT-PEG or 30 µM Y-27632 and loaded with calcein, a vital fluorescent dye. *Scale bar*, 20 µm. **b** Summary graphs showing the median effect of the various treatments on astrocytic morphology, i.e., area, perimeter and form factor. *Number* of astrocytes studied in each condition is given in parentheses in the area graph. *Asterisks* indicate a statistical difference when compared to the untreated/control astrocytes. The other differences are marked by the brackets. Kruskal–Wallis one-way ANOVA (KWA) followed by Dunn's test. *$p < 0.05$, **$p < 0.01$

found that all the cells imaged, untreated ($n = 44$) and treated ($n = 114$) accumulated calcein (Fig. 4a), indicating their viability in culture. To assess the morphological parameters, the calcein images were analyzed to obtain the area and perimeter values of the cells and in turn the form factor (FF), a measure of the circularity or roundness of a cell/object; FF = 1 describes a perfectly round/circular object, while a FF $\approx$ 0 describes a line. We found that the astrocytes treated with SWCNT-PEG assumed a mature morphological phenotype, i.e., SWCNT-PEG caused a significant increase in the area and perimeter of astrocytes and a significant decrease in the FF (reminiscent of cell stellation), while PEG alone did not cause any significant changes in the morphological parameters compared to the untreated astrocytes (Fig. 4b; KWA followed by Dunn's test); these findings are in good agreement with our previous work (Gottipati et al. 2014). Y-27632 echoed SWCNT-PEG effects (Fig. 4b). Taken together, these results show that SWCNT-PEG solute induces morphological changes in astrocytes, similar to those caused by a ROCK inhibitor.

Discussion

In this study, we show that the graft copolymer SWCNT-PEG, when applied to the astrocytes in culture, can increase astrocytic ability to uptake glutamate from the extracellular space. We also showed that SWCNT-PEG causes an increase in the surface GLAST-ir, which was accompanied by an increase in the GFAP-ir and a change in astrocytic morphology.

The Na^+-dependent uptake of glutamate by astrocytes in our culture system predominantly occurs through the glutamate transporter GLAST as per ICC (Fig. 1a), a finding consistent with the previous work using rats at comparable development stage (postnatal day 1) (Furuta et al. 1997). It has been shown previously that the ROCK blockers, such as Y-27632 or fasudil, can upregulate astrocytic glutamate transport by remodeling the actin cytoskeleton in cultured astrocytes (Lau et al. 2011). Indeed, we used Y-27632 as a positive control and showed that the glutamate uptake can be enhanced in our culture system (Fig. 1b). As cystine was not added to the uptake buffer, the recorded Na^+-dependent uptake was not tainted by in parallel operation of the cystine/glutamate antiporter (system x_c^-), a Cl^--dependent system, which would otherwise affect our measurements. Yet, in our experimental conditions, we observed ~40 % block of glutamate uptake by TBOA, which is substantially less than the expected percentage blockage of ~56 %, that we calculated based on a K_i of 42 μM for TBOA and a K_m of 57 μM for L-glutamate for EAAT1/GLAST (Shimamoto et al. 1998). It is possible that this discrepancy is a result of an in parallel Ca^{2+}-dependent glutamate release from astrocytes. Namely, as the added tritiated L-glutamate behaves exactly like native L-glutamate in all signaling and metabolic cellular processes, it binds to plasmalemmal glutamate receptors, leading to an increase in intracellular Ca^{2+} levels and consequential glutamate release (Bezzi et al. 1998). Albeit out of the scope of the present work, such possibility could be discerned by using tritiated D-aspartate which behaves like L-glutamate on plasmalemmal transporters as well as in release from the vesicular pool, but it has a negligible effect on the glutamate receptors compared to that of L-glutamate (Drejer et al. 1986). Nonetheless, SWCNT-PEG enhanced the ability of astrocytes to remove extracellular glutamate (Fig. 1b), which could explain some of the previously observed beneficial effects of this material when applied at the site of spinal cord injury (Roman et al. 2011). Perhaps, SWCNTs reduced the accumulation of extracellular glutamate otherwise leading to excitotoxicity and neuronal death that can occur at the site of neural tissue injury (Choi 1994; Nilsson et al. 1990).

SWCNT-PEG also caused an increase in the surface GLAST-ir (Fig. 2b) as well as the total GFAP-ir (Fig. 3b). Since the loss of astrocyte-specific intermediate filaments, GFAP and vimentin, has hampered vesicular trafficking (Potokar et al. 2007) and the loss of GFAP in particular led to a reduced trafficking of glutamate transporters to the surface of astrocytes (Hughes et al. 2004), it is plausible that an increase in GFAP-ir due to SWCNT-PEG leads to an increase in the trafficking of glutamate transporters to the plasma membrane, which can in turn increase the uptake of glutamate. In addition to this, an increase in GFAP levels is correlated with an increase in the levels of glutamine synthetase (Wang and Hatton 2009; Wang et al. 2013), an enzyme that converts glutamate to glutamine in astrocytes, and an increased glutamine synthetase expression leads to an increase in glutamate uptake and glutamine release (Zou et al. 2010). Unlike glutamate, glutamine released into the extracellular space does not stimulate the receptors present on the neurons, pointing to an additional possible mechanism by which CNTs may mediate beneficial effects in neuroprosthesis applications, e.g., treatment of injury, with glutamate-mediated excitotoxicity settings in place.

Expectedly, along with an increase in GFAP-ir, SWCNT-PEG also caused a change in the morphology of astrocytes, making astrocytes larger and stellate (Fig. 4b); these findings are consistent with our previous work (Gottipati et al. 2012, 2014). It should be noted that, albeit confirmatory, these experiments were a necessary control to accommodate for the batch-to-batch variability in SWCNT-PEG synthesis and to make a comparison with the effects caused by Y-27632, which were reminiscent of the effects induced by SWCNT-PEG (Figs. 3, 4). These similarities might suggest that the mechanism of action of SWCNT-PEG to induce

morphological changes in astrocytes could involve the Rho/ROCK pathway.

In the present study, we used SWCNT-PEG at a concentration of 5 μg/ml for 4 days in culture and found no adverse effects on astrocytes. However, the effects of these carbon materials at varying concentrations and exposure times are currently unknown. As some concerns on their possible toxicity and biological incompatibility have been raised (Belyanskaya et al. 2009; Wick et al. 2007), much needed exposure limits need to be set in place in order to bring the use of CNTs into the realm of neural prosthesis.

Acknowledgments We thank Stephanie M. Robert and Dr. Harald Sontheimer, University of Alabama at Birmingham, for their help with the glutamate uptake study and Dr. Vladimir Grubišić for his constructive comments on a previous version of this manuscript. V. Parpura acknowledges the support of this work by National Institutes of Health (The Eunice Kennedy Shriver National Institute of Child Health and Human Development award HD078678).

Conflict of interest The authors declare that they have no conflict of interest.

Ethical standard All applicable international, national and/or institutional guidelines for the care and use of animals were followed. All procedures performed in studies involving animals were in accordance with the ethical standards of the institution or practice at which the studies were conducted.

References

Abe K, Misawa M (2003) Astrocyte stellation induced by Rho kinase inhibitors in culture. Brain Res Dev Brain Res 143:99–104

Aprico K, Beart PM, Crawford D, O'Shea RD (2004) Binding and transport of [3H](2S,4R)- 4-methylglutamate, a new ligand for glutamate transporters, demonstrate labeling of EAAT1 in cultured murine astrocytes. J Neurosci Res 75:751–759. doi:10.1002/jnr.20013

Bekyarova E, Ni Y, Malarkey EB, Montana V, McWilliams JL, Haddon RC, Parpura V (2005) Applications of carbon nanotubes in biotechnology and biomedicine. J Biomed Nanotechnol 1:3–17. doi:10.1166/jbn.2005.004

Belyanskaya L, Weigel S, Hirsch C, Tobler U, Krug HF, Wick P (2009) Effects of carbon nanotubes on primary neurons and glial cells. Neurotoxicology 30:702–711. doi:10.1016/j.neuro.2009.05.005

Bezzi P et al (1998) Prostaglandins stimulate calcium-dependent glutamate release in astrocytes. Nature 391:281–285. doi:10.1038/34651

Brenner M (2014) Role of GFAP in CNS injuries. Neurosci Lett 565:7–13. doi:10.1016/j.neulet.2014.01.055

Chang SY, Shon YM, Agnesi F, Lee KH (2009) Microthalamotomy effect during deep brain stimulation: potential involvement of adenosine and glutamate efflux. Conf Proc IEEE Eng Med Biol Soc 2009:3294–3297. doi:10.1109/IEMBS.2009.5333735

Choi DW (1994) Glutamate receptors and the induction of excitotoxic neuronal death. Prog Brain Res 100:47–51

Drejer J, Honore T, Meier E, Schousboe A (1986) Pharmacologically distinct glutamate receptors on cerebellar granule cells. Life Sci 38:2077–2085

Drummond GB (2009) Reporting ethical matters in the journal of physiology: standards and advice. J Physiol 587:713–719. doi:10.1113/jphysiol.2008.167387

Furuta A, Rothstein JD, Martin LJ (1997) Glutamate transporter protein subtypes are expressed differentially during rat CNS development. J Neurosci 17:8363–8375

Gottipati MK, Kalinina I, Bekyarova E, Haddon RC, Parpura V (2012) Chemically functionalized water-soluble single-walled carbon nanotubes modulate morpho-functional characteristics of astrocytes. Nano Lett 12:4742–4747. doi:10.1021/nl302178s

Gottipati MK, Bekyarova E, Brenner M, Haddon RC, Parpura V (2014) Changes in the morphology and proliferation of astrocytes induced by two modalities of chemically functionalized single-walled carbon nanotubes are differentially mediated by glial fibrillary acidic protein. Nano Lett 14:3720–3727. doi:10.1021/nl4048114

Hua X, Malarkey EB, Sunjara V, Rosenwald SE, Li WH, Parpura V (2004) Ca^{2+}-dependent glutamate release involves two classes of endoplasmic reticulum Ca^{2+} stores in astrocytes. J Neurosci Res 76:86–97

Hughes EG, Maguire JL, McMinn MT, Scholz RE, Sutherland ML (2004) Loss of glial fibrillary acidic protein results in decreased glutamate transport and inhibition of PKA-induced EAAT2 cell surface trafficking. Brain Res Mol Brain Res 124:114–123. doi:10.1016/j.molbrainres.2004.02.021

Keefer EW, Botterman BR, Romero MI, Rossi AF, Gross GW (2008) Carbon nanotube coating improves neuronal recordings. Nat Nanotechnol 3:434–439. doi:10.1038/nnano.2008.174

Lau CL, O'Shea RD, Broberg BV, Bischof L, Beart PM (2011) The Rho kinase inhibitor Fasudil up-regulates astrocytic glutamate transport subsequent to actin remodelling in murine cultured astrocytes. Br J Pharmacol 163:533–545. doi:10.1111/j.1476-5381.2011.01259.x

Malarkey EB, Parpura V (2007) Applications of carbon nanotubes in neurobiology. Neurodegener Dis 4:292–299. doi:10.1159/000101885

Malarkey EB, Ni Y, Parpura V (2008) Ca^{2+} entry through TRPC1 channels contributes to intracellular Ca^{2+} dynamics and consequent glutamate release from rat astrocytes. Glia 56:821–835. doi:10.1002/glia.20656

McCarthy KD, de Vellis J (1980) Preparation of separate astroglial and oligodendroglial cell cultures from rat cerebral tissue. J Cell Biol 85:890–902

Montana V, Ni Y, Sunjara V, Hua X, Parpura V (2004) Vesicular glutamate transporter-dependent glutamate release from astrocytes. J Neurosci 24:2633–2642. doi:10.1523/JNEUROSCI.3770-03.2004

Ni Y, Hu H, Malarkey EB, Zhao B, Montana V, Haddon RC, Parpura V (2005) Chemically functionalized water soluble single-walled carbon nanotubes modulate neurite outgrowth. J Nanosci Nanotechnol 5:1707–1712

Nilsson P, Hillered L, Ponten U, Ungerstedt U (1990) Changes in cortical extracellular levels of energy-related metabolites and amino acids following concussive brain injury in rats. J Cereb Blood Flow Metab 10:631–637

Park E, Velumian AA, Fehlings MG (2004) The role of excitotoxicity in secondary mechanisms of spinal cord injury: a review with an emphasis on the implications for white matter degeneration. J Neurotrauma 21:754–774. doi:10.1089/0897715041269641

Potokar M et al (2007) Cytoskeleton and vesicle mobility in astrocytes. Traffic 8:12–20

Reyes RC, Perry G, Lesort M, Parpura V (2011) Immunophilin deficiency augments Ca^{2+}-dependent glutamate release from mouse cortical astrocytes. Cell Calcium 49:23–34

Roman JA, Niedzielko TL, Haddon RC, Parpura V, Floyd CL (2011) Single-walled carbon nanotubes chemically functionalized with polyethylene glycol promote tissue repair in a rat model of spinal cord injury. J Neurotrauma 28:2349–2362. doi:10.1089/neu.2010.1409

Sage D, Neumann FR, Hediger F, Gasser SM, Unser M (2005) Automatic tracking of individual fluorescence particles: application to the study of chromosome dynamics. IEEE Trans Image Process 14:1372–1383

Shimamoto K, Lebrun B, Yasuda-Kamatani Y, Sakaitani M, Shigeri Y, Yumoto N, Nakajima T (1998) DL-threo-beta-benzyloxyaspartate, a potent blocker of excitatory amino acid transporters. Mol Pharmacol 53:195–201

Wang YF, Hatton GI (2009) Astrocytic plasticity and patterned oxytocin neuronal activity: dynamic interactions. J Neurosci 29:1743–1754. doi:10.1523/JNEUROSCI.4669-08.2009

Wang YF, Sun MY, Hou Q, Parpura V (2013) Hyposmolality differentially and spatiotemporally modulates levels of glutamine synthetase and serine racemase in rat supraoptic nucleus. Glia 61:529–538. doi:10.1002/glia.22453

Wick P et al (2007) The degree and kind of agglomeration affect carbon nanotube cytotoxicity. Toxicol Lett 168:121–131. doi:10.1016/j.toxlet.2006.08.019

Wilms H, Hartmann D, Sievers J (1997) Ramification of microglia, monocytes and macrophages in vitro: influences of various epithelial and mesenchymal cells and their conditioned media. Cell Tissue Res 287:447–458

Zou J, Wang YX, Dou FF, Lu HZ, Ma ZW, Lu PH, Xu XM (2010) Glutamine synthetase down-regulation reduces astrocyte protection against glutamate excitotoxicity to neurons. Neurochem Int 56:577–584